Molecular Phylogenetics and Evolution 94 (2016) 605–617

Contents lists available at ScienceDirect

Molecular Phylogenetics and Evolution

journal homepage: www.elsevier.com/locate/ympev

Utilizing next-generation sequencing to resolve the backbone of the Core Goodeniaceae and inform future taxonomic and floral form studies ☆

Andrew G. Gardner [a,*,1], Emily B. Sessa [b,c,1], Pryce Michener [a], Eden Johnson [a], Kelly A. Shepherd [d], Dianella G. Howarth [e], Rachel S. Jabaily [a]

[a] Department of Biology, Rhodes College, Memphis, TN 38112, USA
[b] Department of Biology, University of Florida, Gainesville, FL 32607, USA
[c] Genetics Institute, University of Florida, Gainesville, FL 32607, USA
[d] Western Australian Herbarium, Department of Parks and Wildlife, Kensington, WA 6151, Australia
[e] Department of Biological Sciences, St. John's University, Queens, NY 11439, USA

ARTICLE INFO

Article history:
Received 16 April 2015
Revised 18 September 2015
Accepted 2 October 2015
Available online 20 October 2015

Keywords:
Backbone topology
Goodeniaceae
Goodenia
Nuclear ribosomal repeat
Plastome
Scaevola

ABSTRACT

Though considerable progress has been made in inferring phylogenetic relationships of many plant lineages, deep unresolved nodes remain a common problem that can impact downstream efforts, including taxonomic decision-making and character reconstruction. The Core Goodeniaceae is a group affected by this issue: data from the plastid regions *trnL-trnF* and *matK* have been insufficient to generate adequate support at key nodes along the backbone of the phylogeny. We performed genome skimming for 24 taxa representing major clades within Core Goodeniaceae. The plastome coding regions (CDS) and nuclear ribosomal repeats (NRR) were assembled and complemented with additional accessions sequenced for nuclear G3PDH and plastid *trnL-trnF* and *matk*. The CDS, NRR, and G3PDH alignments were analyzed independently and topology tests were used to detect the alignments' ability to reject alternative topologies. The CDS, NRR, and G3PDH alignments independently supported a *Brunonia* (*Scaevola* s.l. (*Coopernookia* (*Goodenia* s.l.))) backbone topology, but within *Goodenia* s.l., the strongly-supported plastome topology (*Goodenia* A (*Goodenia* B (*Velleia* + *Goodenia* C))) contrasts with the poorly supported nuclear topology ((*Goodenia* A + *Goodenia* B) (*Velleia* + *Goodenia* C)). A fully resolved and maximally supported topology for Core Goodeniaceae was recovered from the plastome CDS, and there is excellent support for most of the major clades and relationships among them in all alignments. The composition of these seven major clades renders many of the current taxonomic divisions non-monophyletic, prompting us to suggest that *Goodenia* may be split into several segregate genera.

1. Introduction

As molecular phylogenetic analyses of large plant clades have become more common, many have encountered a recurrent problem: major clades are resolved with strong support, but clear, well-supported relationships among those clades is lacking ("backbone topologies," e.g., Wurdack and Davis, 2009; Refulio-Rodriguez and Olmstead, 2014; Straub et al., 2014). Resolution of such topologies often has critical implications for character-state inference and taxonomic decisions involving the tip taxa. This challenge of clarifying recalcitrant backbones is usually attributed to the fact that many angiosperm clades are the consequence of ancient, rapid radiations (Rokas and Carroll, 2006; Whitfield and Lockhart, 2007) that result in extremely short branches, and which require analysis of tens of thousands of base pairs for resolution (e.g., Jian et al., 2008; Wang et al., 2009; Barrett et al., 2014; Straub et al., 2014).

A common approach to resolve such issues has been to add more taxa and loci via Sanger sequencing, ideally from multiple genomic compartments. The success of such projects is often limited by factors of time, money, and access to high quality DNA, and frequently only yields incremental increases in support. High throughput, or next generation, sequencing (hereafter referred to as NGS) techniques offer the promise of dramatically-increased volumes of sequence data to address these issues (Soltis et al., 2010, see also *American Journal of Botany*, volume 99) and have been used with increasing frequency to resolve nodes that

☆ This paper was edited by the Associate Editor Elizabeth Zimmer.

* Corresponding author.
E-mail address: andyggardner@gmail.com (A.G. Gardner).

[1] These authors contributed equally to this work.

http://dx.doi.org/10.1016/j.ympev.2015.10.003
1055-7903/

persistently received low support with Sanger data (e.g., Givnish et al., 2010; Moore et al., 2010; Straub et al., 2012; Barrett et al., 2014; Eserman et al., 2014). Factors to consider when employing this approach include scalability, library quality, and previous investment in Sanger data generation. Multiplex barcodes that allow for pooling dozens or even hundreds of accessions per lane increase the feasibility of scaling NGS approaches to taxon-rich datasets. However, researchers working within large clades may be limited by sampling issues, particularly if relying on lower-quality DNA sourced predominantly from herbarium material, as degraded tissues may reduce library quality, compromising downstream sequencing and assembly. Moreover, many labs have already invested heavily in generating large amounts of Sanger data over the years, which may have been sufficient to establish relationships within major clades. A hybrid NGS and Sanger approach is a promising tactic in such situations, as it utilizes existing Sanger data to evaluate relationships between close relatives, and permits efficient use of NGS for targeted taxa in key phylogenetic positions as representatives of well-supported clades or key nodes. The NGS data are expected to produce a well-supported topological backbone, which can then be applied, for example, as a topological constraint in analyses of an expanded-taxon, Sanger-sequenced data set, or the two datasets can be analyzed together in a combined matrix. Such approaches have been applied successfully in several groups to date, including hyalid frogs (Wiens et al., 2005), *Agama* lizards (Leaché et al., 2014), butterflies and moths (Cho et al., 2011), temperate bamboos (Ma et al., 2014), Malpighiales (Xi et al., 2012), and monocots (Davis et al., 2013).

This hybrid method may be useful in resolving the backbone of the Australian fan-flower family Goodeniaceae. Goodeniaceae are sister to the major angiosperm clade Asteraceae plus Calyceraceae (Tank and Donoghue, 2010), and like several other members of the Asterales, have evolved secondary pollen presentation. In Goodeniaceae, this occurs via a cup-like stylar indusium, the synapomorphy of the family. The 420+ species are principally endemic to Australia, with multiple radiations of the genus *Scaevola* in Pacific island systems (Howarth et al., 2003; Jabaily et al., 2014). Phylogenetic analyses (Jabaily et al., 2012) of 3100 aligned base pairs from the fast evolving plastid locus *trnL-trnF* and the slower evolving *matK* for half of the described species resolved the major clade Core Goodeniaceae sister to the smaller 'LAD' clade comprising *Lechenaultia* R.Br (*Anthotium* R.Br. + *Dampiera* R.Br.). Core Goodeniaceae in turn is composed of two major sister lineages, *Goodenia* s.l. (including the genera *Coopernookia* Carolin, *Goodenia* Sm., *Selliera* Cav., *Velleia* Sm., *Verreauxia* Benth., and *Pentaptilon* E.Pritzel) and *Scaevola* (+*Diaspasis* R.Br.), together sister to the monotypic *Brunonia australis* R.Br. Multiple major clades were recovered with strong support within *Goodenia* s.l., including three principal clades of a paraphyletic *Goodenia*; however, some backbone relationships received weak support. The three clades (A, B, C) broadly represented infrageneric groups currently recognized within the genus (Table A). Placed as sister with low support to the small genus *Coopernookia*, clade A included the generic type species *G. ovata* Sm., most members of subg. *Goodenia* Sm. subsect. *Goodenia* Sm., *Scaevola collaris* F. Muell. and the monotypic genus *Selliera*. The majority of representatives of clade B included members of subsect. *Ebracteolatae* K. Krause and one species of subsect. *Borealis* Carolin. Sister to well-supported *Velleia*, clade C was comprised of morphologically diverse groups encompassing some additional members of subsect. *Goodenia*, subg. *Monochila* (G. Don) Carolin, subsections *Coeruleae* (Benth.) Carolin and *Scaevolina* Carolin, along with the depauperate southwestern Australian genera *Verreauxia* and *Pentaptilon*. Analysis of highly variable regions of *trnL-trnF* within *Goodenia* s.l. that were previously excluded from family-wide analysis because of issues with alignment did increase phylogenetic support in some of these poorly supported or unresolved nodes; however, a fully resolved and supported backbone for *Goodenia* s.l. was not recovered and potential alternate histories from nuclear markers were not explored. This is a prime example of the limitations of sequencing few loci for phylogenetic resolution along the backbone of a clade. Even without a fully resolved phylogeny, it was clear that major generic-level taxonomic changes were required but we could not seek to make changes to *Goodenia* s.l. without consistent resolution of the backbone relationships and confidence in the species-level composition of each major clade. Clarifying the relationships among *Goodenia* clades A, B, C and the smaller affiliate genera is necessary to identify monophyletic groups and facilitate the investigation of the morphological synapomorphies that distinguish them, and to ensure that currently undescribed, informally phrase-named taxa (e.g. *Goodenia* sp. Stirling Range (R. Cranfield & D. Kabay 9148), Western Australian Herbarium, 1998) will be originally authored within the appropriate clades.

Calibration of the Core Goodeniaceae phylogeny against geological time found that the *Goodenia* s.l. backbone branches are relatively short, with all of the major extant clades diverging by the earliest Miocene (~23 mya; Jabaily et al., 2014). The sister clade *Scaevola* s.l. underwent a much more recent, rapid crown radiation starting in the mid-Miocene (~14 mya) both in Australia and repeatedly in the Pacific Islands, most notably via multiple introductions to Hawaii. Phylogenetic resolution is minimal within *Scaevola* s.l., with support for a small clade sister to the remainder, and some smaller clades of island endemics. Species-level relationships of Hawaiian *Scaevola* were studied using multiple plastid and nuclear loci to infer dispersal history from Australia (Howarth et al., 2003) and to identify the homoploid hybrid origins of several Hawaiian species (Howarth and Baum, 2005). Conflict between low-copy nuclear loci and nrITS was only found in cases of homoploid hybridization, with concordance for all other relationships.

Given the persistent low support and recalcitrance of the backbone topology in Core Goodeniaceae, we opted to integrate targeted NGS of relatively few taxa with expanded-taxon-set Sanger sequencing in order to resolve the relationships among the major clades in this group. We took a genome skimming approach (Straub et al., 2012; Bock et al., 2014) to the NGS aspect of this study, in order to generate data from plastid and nuclear genomic compartments, and because initial time and monetary investment was lower than for Hyb-seq or other methods that require probe development (Weitemier et al., 2014). Here, data generated via this approach are presented from plastid genomes (plastomes) and the nuclear ribosomal repeat (NRR), as well as three other expanded-taxon-set Sanger-sequenced datasets. We selected 24 key taxa representing well-supported clades within Core Goodeniaceae (*sensu* Jabaily et al., 2012) for genome skimming, and assembled plastome coding sequences and NRRs for this set of taxa from the resulting NGS sequence data. We compared these data with Sanger-generated assemblies for the nuclear marker Glyceraldehyde 3-Phosphate Dehydrogenase (G3PDH; Strand et al., 1997). Finally, we implemented two analyses that linked the plastome data with our existing Sanger-generated plastid data to enhance phylogenetic resolution. One analysis concatenated the plastome data with a 98-taxon dataset for *trnL-trnF* and *matK*, and the second analysis used the plastome topology as a constraint on the 98-taxon dataset. We use these various datasets and subsequent analyses to address the following questions: (1) Can draft plastomes generated via NGS resolve with high support the backbone of Core Goodeniaceae? (2) Have the plastome, G3PDH, and NRR tracked similar or different evolutionary histories? (3) Can constraining a Sanger dataset to the plastome topology or concatenating the Sanger and plastome datasets result in phylogenetic resolution at all depths? (4) What future taxonomic changes are warranted by the resulting topologies?

2. Materials and methods

2.1. Taxon sampling and DNA extraction

Taxa were sampled for inclusion in three accession sets. The first included accessions of 24 species that represent the major clades of *Goodenia* s.l. and *Scaevola* s.l. *sensu* Jabaily et al. (2012), which were sequenced via genome-skimming (Table B). Twenty-four accessions were included as this allowed us to adequately represent the major clades while using the number of barcodes available in our selected NGS library preparation kit (see below). All plant material for this accession set was collected in the field or from cultivated specimens, preserved in silica gel, and vouchered at PERTH. The second accession set comprised 35 accessions representing an expanded sampling within the major clades of *Goodenia* s.l. These were Sanger sequenced for the nuclear gene G3PDH. The third accession set included 98 species across Core Goodeniaceae that we Sanger sequenced for *trnL-trnF* and *matK*. This includes 135 newly-generated sequences and 59 sequences from Jabaily et al. (2012). Because we did not want our phylogenetic results to be influenced by accessions with missing data, we elected to retain only the accessions for which we had complete sequences of both of these loci. This resulted in the non-inclusion of some taxa that were included in Jabaily et al. (2012), including *Pentaptilon*. Material from additional taxa included in the G3PDH and plastid datasets was taken from herbarium vouchers (Appendix A). For all accessions total DNA was extracted using the Qiagen DNeasy Plant Mini Kit (Valencia, California, USA), following the manufacturer's protocols except that, for NGS library preparation 30 μL elution buffer was used to maximize DNA concentration.

2.2. NGS sequencing, assembly, and alignment

We constructed Illumina libraries using the Nextera DNA Sample Preparation Kit (Illumina, San Diego, California). Barcodes were added to allow for multiplexing, and size-selection was performed targeting regions 500–600 base pairs (bp) in length. Prior to sequencing, libraries underwent quality control and validation using the Agilent Bioanalyzer and qPCR according to Illumina's Quantification Protocol Guide. The 24 libraries were multiplexed in equimolar ratios and sequenced in two lanes (all libraries sequenced in both lanes to maximize redundancy) on an Illumina Hiseq 2500 rapid run with 150 bp paired-end chemistry. Sequencing and pre- and post-run quality control were performed by Macrogen (Macrogen, Seoul, South Korea), and reads passing Illumina's standard quality filters were retained for assembly following additional quality control assessment with FastQC (http://www.bioinformatics.bbsrc.ac.uk/projects/fastqc/).

We assembled draft plastid genomes using *Helianthus annuus* L. (NC_007977; Timme et al., 2007) as a reference, after first removing one copy of the inverted repeat (following Straub et al., 2012, 2014). We performed reference-guided assembly in Geneious Pro 7.1 (Biomatters, Auckland, New Zealand) using the medium sensitivity algorithm and up to five iterations. Annotations were transferred from *H. annuus* to Goodeniaceae plastomes if they shared at least 65% sequence identity. We removed intergenic regions prior to alignment in order to produce a concatenated data matrix consisting only of protein-coding genes (hereafter referred to as the CDS dataset). The *H. annuus* reference was included in the matrix as an outgroup, and alignment was performed using MAFFT v7.149b with default settings (Katoh and Standley, 2013). We used PartitionFinder (http://www.robertlanfear.com/partitionfinder/) to identify the optimal model of molecular evolution for each gene, and the optimal partitioning scheme for the CDS dataset as a whole, using the BIC (Bayesian Information Criterion) option.

The NRR was assembled following a similar protocol, except that we used a different *H. annuus* accession (KF767534; Bock et al., 2014). For some taxa, medium sensitivity setting of the Geneious assembly algorithm failed to reconstruct conserved regions in the external transcribed spacer. For these, the high sensitivity algorithm was used to generate a second sequence and both were included in downstream analyses to check for taxon monophyly. Regions with less than 25x coverage were removed from the consensus sequences. The ribosomal repeats were aligned in Geneious using its implementation of MUSCLE (Edgar, 2004), with 8 iterations. We used jModelTest2 (Darriba et al., 2012) to identify the optimal model of evolution for the NRR.

2.3. Sanger sequencing and alignment

Amplifications of *trnL-trnF* and *matK* followed Jabaily et al. (2012). Amplification of G3PDH followed Howarth and Baum (2005) and yielded single bands that were directly sequenced. All sequencing was performed by Macrogen. We assembled chromatograms, generated consensus sequences, and performed alignment using Geneious Pro 7.1. Following alignment by the built-in Geneious aligner under standard settings (65% similarity cost matrix, gap opening penalty of 12 and gap extension penalty of 3), we manually adjusted the alignments following a similarity criterion (e.g., Simmons, 2004) prior to concatenating the two loci and running phylogenetic analyses. We used jModelTest2 (Darriba et al., 2012) to identify the optimal model(s) of evolution for *trnL-trnF*, *matK*, and G3PDH.

2.4. Phylogenetic analyses

We performed maximum parsimony (MP), maximum likelihood (ML), and Bayesian inference (BI) phylogenetic analyses on the four primary datasets: (1) plastome CDS for 24 taxa, (2) NRR for 24 taxa, (3) nuclear G3PDH for 35 taxa, and (4) plastid loci *trnL-trnF* and *matK* for 98 taxa. For the plastome CDS dataset, we used two partitioning schemes: the best scheme recommended by PartitionFinder on a gene-by-gene basis, and all genes concatenated and partitioned by codon position. The second dataset was analyzed with all three codon positions at once, partitioned separately, and also in three separate analyses, each with only one codon position present.

Maximum parsimony bootstrap (MP BS) analyses for each dataset were performed in PAUP* 4.0a136 (Swofford, 2002) with 1000 replicates, each with 100 random taxon-addition starting trees, TBR branch-swapping, and multrees on, limiting the rearrangements to 10,000,000. Maximum likelihood (ML) analyses were performed with RAxML v. 8.0.0 (Stamatakis, 2014), using the optimal model(s) of molecular evolution and the optimal partitioning schemes identified for each dataset. We conducted a rapid bootstrap analysis with 1000 replicates and searched for the best-scoring ML tree in a single run (option "-f a"), and then used SumTrees v3.3.1 (Sukumaran and Holder, 2010) to summarize bootstrap support on the best ML topology for each dataset. We conducted BI analyses using the MPI version of MrBayes 3.2.1 (Ronquist and Huelsenbeck, 2003; Altekar et al., 2004), with two independent runs of 20 million generations and four chains per run, sampling trees every 1000 generations. We used a chain temp of 0.2 and uniform priors. Optimal partitioning schemes were also used in all MrBayes runs. Chain convergence, stationarity, and estimated sample size (ESS) were assessed in Tracer 1.6 (Rambaut et al., 2014) by visually examining plots of parameter values and log-likelihood against the number of generations. Convergence and stationarity were assumed when the average standard

deviation of split frequencies reached 0.01 or less, and ESS was considered satisfactory when the recommended threshold of 200 had been passed (Drummond and Rambaut, 2007). For each dataset, we discarded the first 25% of trees from each run as burn-in, and the remaining trees from the two runs were combined and annotated using TreeAnnotator v1.8.0 (part of the BEAST package; Drummond et al., 2012). ML and BI analyses were conducted on the high performance computing cluster (HiPerGator) at the University of Florida.

To assess incongruence between the CDS, NRR, and nuclear G3PDH datasets, we implemented partition homogeneity tests for all combinations of alignments (ILD test; Farris et al., 1994), using 1000 replicates with the same heuristic search criteria used in the bootstrap analyses. To test the hypothesis that the CDS alignment can statistically reject a backbone topology generated by the NRR and G3PDH alignments ((*Goodenia* A + *Goodenia* B) (*Velleia* + *Goodenia* C)), and that the NRR and G3PDH alignments cannot statistically reject the backbone generated by the CDS alignment (*Goodenia* A (*Goodenia* B (*Velleia* + *Goodenia* C))), we used three Shimodaira Approximately-Unbalanced (AU) tests (Shimodaira, 2002, implemented in PAUP*), each with 1000 resampling of estimated log-likelihoods (RELL) bootstraps, to assess whether the constrained maximum likelihood topologies (and branch lengths) are significantly worse than the unconstrained ones.

Finally, we analyzed a fourth dataset, comprised of complete Sanger-generated sequences for 98 taxa of *trnL-trnF* and *matK*, with which to compare two methods for incorporating the plastome CDS dataset—concatenation and constraint. After removing *matK* from the CDS alignment, we concatenated it to the 98-taxon dataset. Additionally, we used the best ML topology from analysis of the 24-taxon CDS matrix as a constraint (on just those 24 taxa) during analysis of the 98-taxon dataset. The constraint was imposed using the "-r" option in RAxML, a set of constraint clades in MrBayes (a "partial" constraint), and a "backbone" constraint in PAUP*. We conducted ML, Bayesian, and parsimony analyses on these datasets as above. All datasets are publicly available on Dryad (http://dx.doi.org/10.5061/dryad.4mp00).

3. Results

3.1. Assembly and phylogenetic analyses of plastome data

Sequencing on the Illumina HiSeq 2500 produced between 14 and 24 million paired-end (2 × 150 bp) reads per species (mean 19 million; Table B). An average of 567,000 (3%) of these reads mapped to the plastome during reference-guided assemblies. Mean assembly length was 139,377 bp, with average depth of coverage ranging from 228 to 1967 (mean 694×). The *Helianthus annuus* plastome used to guide assembly of the Goodeniaceae plastomes contains 81 unique protein coding genes (84,209 bp; Timme et al., 2007). Of these, 11 did not assemble for any Goodeniaceae species; these include several genes known to be polymorphic even between close relatives *Helianthus* L. and *Lactuca* L. (Timme et al., 2007). Of the remaining 70 genes, 48 were present in all Goodeniaceae species and 22 were present in only some species. For these 22 genes with partial coverage, missing genes were distributed randomly among both taxa and genes. In the matrix overall, there was 94% coverage of the 70 assembled genes across the 24 Goodeniaceae species, and 8% missing data at the nucleotide level. The final aligned CDS data matrix, including *H. annuus*, was 52,388 bp in length, with 10.1% parsimony informative characters.

Maximum parsimony, maximum likelihood, and Bayesian analyses of the CDS dataset produced identical tree topologies, with 100% bootstrap support (BS) from MP and ML analyses and 1.0 Bayesian posterior probabilities (PP) at almost every node. The trees produced by separate analyses of the CDS dataset partitioned by gene and/or codon position produced identical topologies with similarly high support values. The best ML topology from analysis of the complete, concatenated CDS dataset ($\ln L = -221{,}235.92$) is shown (Fig. 1; the remaining trees, from the various analyses of codons and/or genes, are not shown, as they are identical to this tree). Only two nodes on very short branches did not receive 100/1.0/100 support (ML-BS/BI-PP/MP-BS), instead receiving 97/1.0/95 (clade within *Goodenia* C) and 79/1.0/86 (clade within *Goodenia* A).

All phylogenies recovered *Brunonia australis* as sister to the remaining Core Goodeniaceae on a long branch, with the remaining taxa split into *Scaevola* s.l. and *Goodenia* s.l., congruent with results from Jabaily et al. (2012). Within *Goodenia* s.l., the major clades of Jabaily et al. (2012) are recovered, but now with strong support for relationships among these clades. The small genus *Coopernookia* is sister to the remainder of *Goodenia* s.l. Within, *Goodenia* A is sister to (*Goodenia* B (*Velleia* + *Goodenia* C)). In *Goodenia* C, *Goodenia hassallii* F. Muell. of subsect. *Coeruleae* (referred to as 'C-C') diverges first, from a clade composed of *Verreauxia* ('C-V') plus members of *Goodenia* subg. *Monochila* ('C-M').

3.2. Assembly and phylogenetic analyses of nuclear ribosomal repeat (NRR) data

Reference-guided assemblies under the medium sensitivity algorithm mapped an average of 257,873 reads (1.4%) to the *Helianthus annuus* NRR. Average full assembly length was 7376 bp and average coverage depths ranged from 849 to 79,177, with a mean of 10,029× coverage (Table B). Following alignment, the data matrix was 10,375 bp in length. A few accessions required removal of sections of the assembly with <25× coverage, almost always at the 5′ end of the external transcribed spacer. This included regions in the *H. annuus* external and nontranscribed spacers of more than 1 kb that members of the Goodeniaceae do not have, yielding some extremely ambiguous areas of the alignment. We elected to remove these sections of the alignment, retaining a matrix of 6721 bp with 9.9% parsimony-informative characters (Supplementary Fig. S1). Accessions that were assembled several times, testing different sensitivity settings, always resolved as monophyletic clades in analyses, and ultimately we retained the medium-sensitivity assemblies for these taxa.

Maximum likelihood analysis of the NRR data results in a tree topology that closely mirrors that from the plastome CDS alignment, with the exception of *Goodenia* A and *Goodenia* B resolving as a clade sister to (*Velleia* + *Goodenia* C) in contrast to the CDS topology (Fig. 2 and Supplementary Fig. S2). Throughout, branch lengths (in substitutions per site) are considerably longer than those produced by either of the other datasets. ML bootstrap support of the seven major clades is moderate, but support is much lower along the backbone, with relationships receiving an average of 51% bootstrap support (ranging from 30% to 73%). Bayesian posterior probabilities and maximum parsimony bootstrap scores tended to be higher along the backbone, but these analyses disagreed in the placement of *Velleia*. Bayesian and ML analyses group *Velleia* with *Goodenia* C, mirroring the other datasets, whereas parsimony bootstrap analysis places *Velleia* sister to *Goodenia* B with weak support. *Verreauxia* ('C-V') is sister to all of the remaining *Goodenia* C taxa, with subsect. *Coeruleae* ('C-C') sister to subg. *Monochila* ('C-M').

3.3. Phylogenetic analyses of G3PDH data

The aligned G3PDH matrix was 986 characters in length, with 31.1% parsimony informative characters. Maximum likelihood analysis yielded a best ML tree ($\ln L = -6415.32$) that closely mirrors that from the NRR alignment, with the exception of *Goodenia*

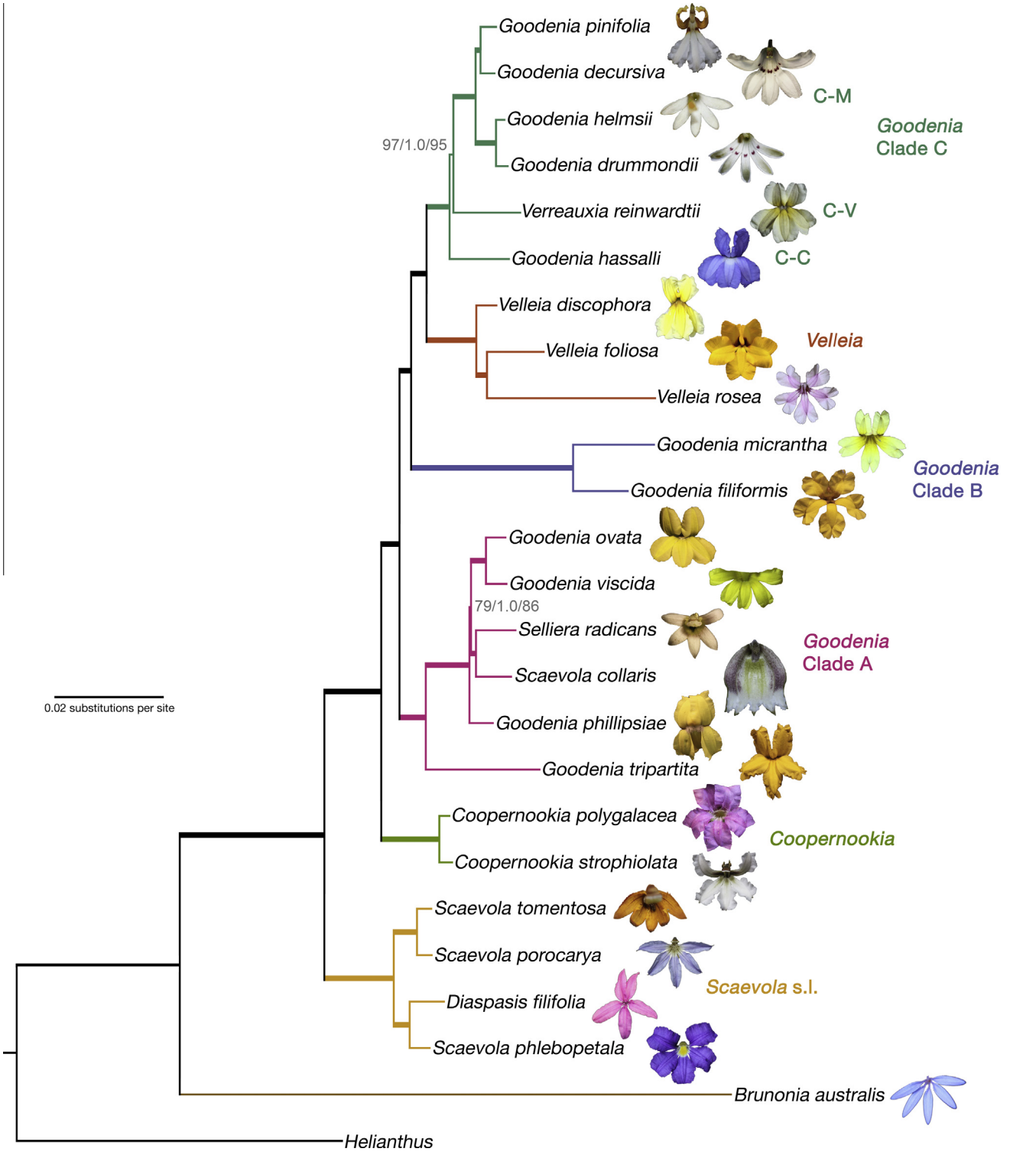

Fig. 1. Best maximum likelihood phylogram resulting from analysis of the CDS dataset for 24 target accessions within Core Goodeniaceae and *Helianthus annuus* as the outgroup. Support values from ML-BS/BI-PP/MP-BS are indicated at two nodes that did not receive maximum support; remaining branches, drawn as thick lines, received 100/1.0/100 support. Note fan-flower morphologies in *Scaevola* s.l., *Goodenia* A, and *Goodenia* C.

A resolving into two clades (labeled A and A′ in Fig. 2 and in Supplementary Fig. S2) successively sister to *Goodenia* B, rather than forming one clade sister to *Goodenia* B. Branch length is generally higher than in the plastome CDS phylogram but shorter than that of the NRR, with the longest branch within *Velleia.* ML bootstrap support values throughout are generally higher than 95%, though the sister relationship of *Goodenia* A′ with *Goodenia* B is weakly supported (50%). Bayesian analysis results in an identical topology, with similarly weak support for the *Goodenia* A′ – *Goodenia* B relationship. Maximum parsimony bootstrap analysis yields a similar topology, except the *Goodenia* A′ – *Goodenia* B relationship only received 34% bootstrap support. In *Goodenia* C, the earliest divergence separates a lineage composed of subgenus *Monochila* ('C-M') from the remaining taxa, with *Verreauxia* ('C-V') then sister

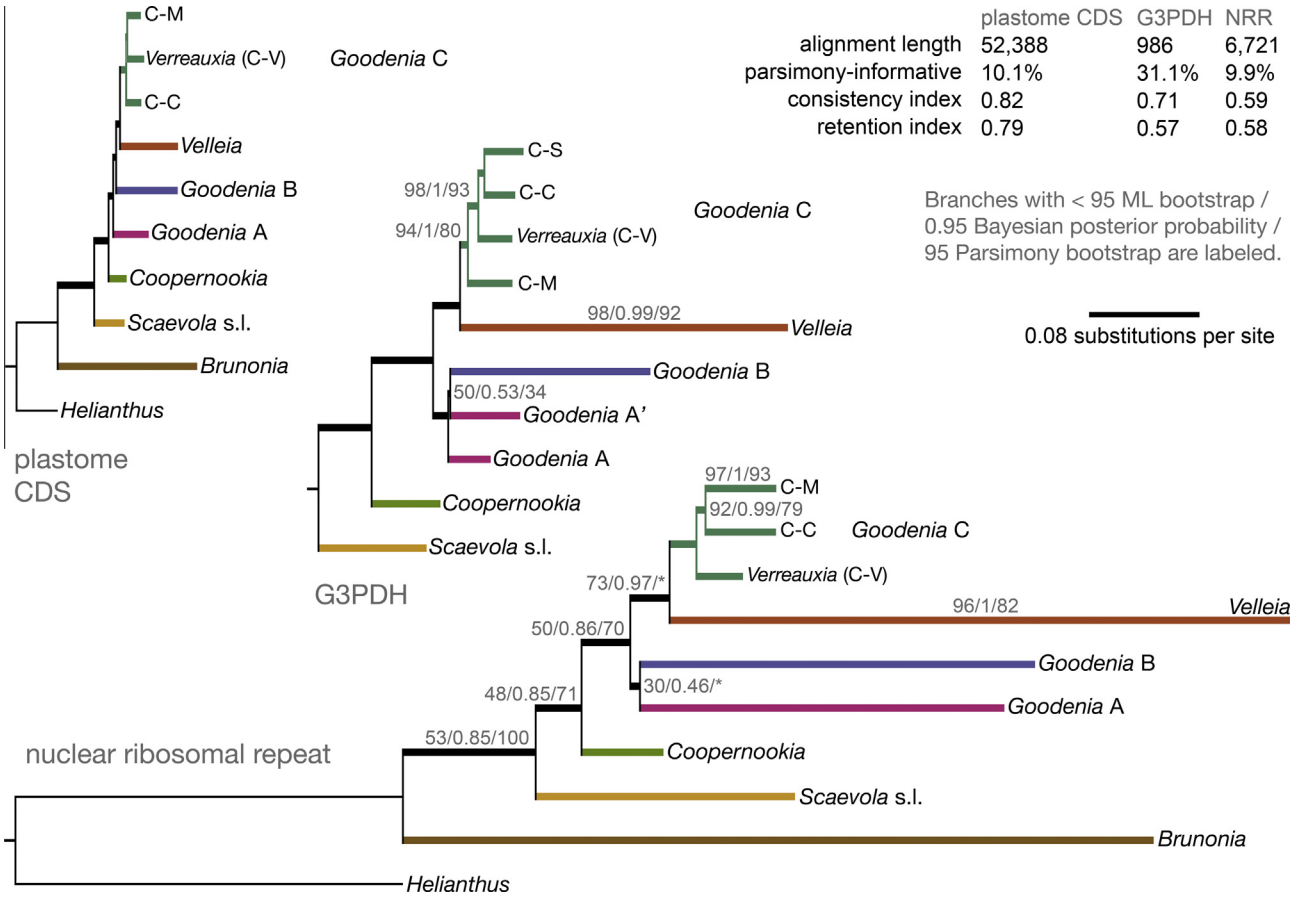

Fig. 2. Simplified best maximum likelihood phylograms resulting from analysis of the CDS, G3PDH, and nuclear ribosomal repeat (NRR) datasets. Support values are ML-BS/BI-PP/MP-BS. When parsimony bootstrap analyses support alternate clades it is denoted with ∗. Terminals reflect the longest branch lengths within the seven focal clades. Alignment lengths, percent parsimony-informative sites, consistency, and retention indices are noted.

to members of subsect. *Coeruleae* ('C-C') plus subsect. *Scaevolina* ('C-S').

3.4. Partition homogeneity tests and Shimodaira Approximately-Unbiased (AU) topology tests

When all three datasets are included, the partition homogeneity test found evidence of significant conflict ($P = 0.001$). Pairwise incongruences exist between nuclear G3PDH and the CDS ($P = 0.012$) and the NRR and the CDS ($P = 0.001$). In contrast, nuclear G3PDH and the NRR do not exhibit significant incongruence ($P = 0.14$). The CDS alignment rejected (at $P = 0.001$) the null hypothesis produced by analyses of the NRR and G3PDH alignments of ((*Goodenia* A + *Goodenia* B) (*Velleia* + *Goodenia* C)). The CDS null hypothesis of (*Goodenia* A (*Goodenia* B (*Velleia* + *Goodenia* C))) was rejected by the G3PDH alignment (at $P = 0.027$) but not by the NRR alignment ($P = 0.197$).

3.5. Constrained and concatenated phylogenetic analysis of Sanger sequenced data

The 98-taxon *trnL-trnF* and *matK* data matrix was 3333 characters in length, with 18.3% parsimony informative characters. The unconstrained, constrained, and concatenated ML analyses produced single best trees with lnLs of −18,943.40, −18,948.67, and −233,819.70 respectively, with support for the seven major clades ranging from 99 to 100 (Fig. 3). The relationships within these major clades were largely congruent with the results of Jabaily et al. (2012). Within *Scaevola* s.l., *Diaspasis filifolia* R.Br. is sister to one representative of sect. *Xerocarpa* G.Don. The relationship of this pair to sect. *Enantiophyllum* Miq. and the remainder of *Scaevola* s.l. is resolved with little confidence. Relationships between other members show sects. *Xerocarpa* and *Scaevola* L. are most likely non-monophyletic, congruent with the findings of the expanded taxon sampling of Jabaily et al. (2012).

In *Goodenia* s.l., the CDS-constrained analyses unsurprisingly lifted many clades' support from the mid and upper 90s in the unconstrained analysis to 100 (Fig. 3). However, the concatenated analysis, in which no constraint was employed, also increased support for many nodes compared to the unconstrained, unconcatenated analysis (Fig. 3). In particular, support for the placement of *Coopernookia* as sister to the remained of *Goodenia* s.l. increased from 61 in the unconstrained, unconcatenated analysis to 100 in the concatenated analysis (it was also 100 in the constrained analysis, where this relationship was enforced).

Goodenia A includes two well-supported clades (A and A′) that receive 100% support in the concatenated analysis. *Goodenia* A incorporates members of subg. *Goodenia*, including the type species *G. ovata*. It also includes *Selliera radicans*, *Scaevola collaris*, *G. phillipsiae* Carolin (subsect. *Ebracteolatae*) and *G. viscida* R.Br. (subg. *Monochila*). *Goodenia* A′ includes only members of subsect. *Goodenia*. *Goodenia B* includes members of sects. *Porphyranthus* G. Don. and *Amphichila* D.C. in a grade sister to the remainder of the species, which are predominantly members of subsect. *Ebracteolatae*, but also includes representatives of series *Borealis* and *Calogyne* (R.Br.) Carolin.*Velleia* is well supported by all analyses in its position sister to *Goodenia* C, which includes several distinct groups. The concatenated analysis maintains the relationship seen

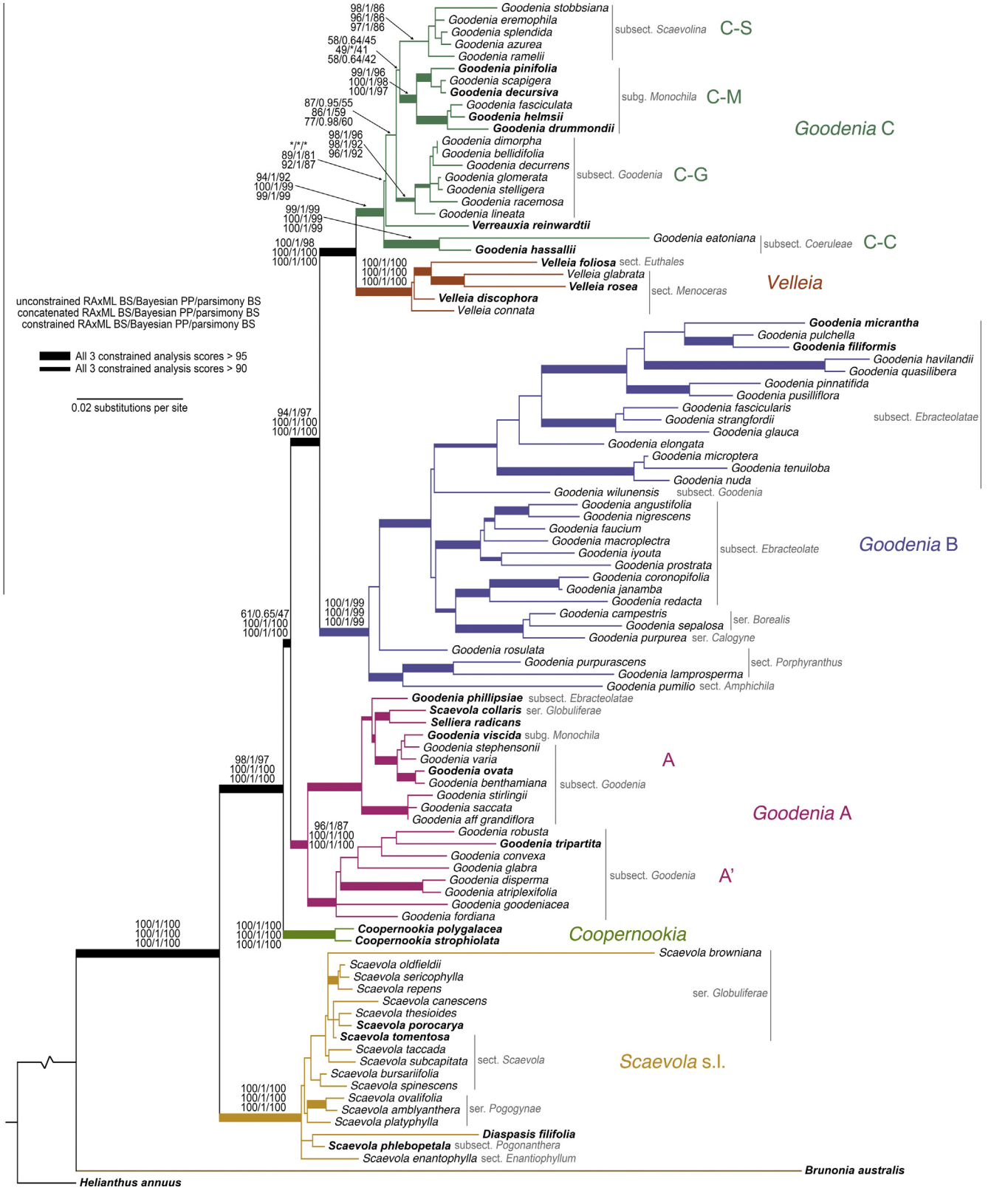

Fig. 3. Best maximum likelihood phylogram resulting from plastome CDS topology-constrained analysis of 98 accession *trnL-trnF* and *matK* alignment. The accessions with NGS data are bold. Key nodes are annotated with support values from ML-BS/BI-PP/MP-BS, with scores above from unconstrained analysis of the same dataset, and constrained scores below. Thickened branches received greater than 95/0.95/95 or 90/0.90/90 in the constrained analyses. When analyses support alternate clades it is denoted with ∗. Accessions are annotated by their current taxonomic classifications. The branch leading to *Helianthus annuus* has been shortened to reduce white space in the figure.

in the CDS dataset (and enforced in the constrained analysis) of subsect. *Coeruleae* ('C-C') sister to the remainder of *Goodenia* C, including *Verreauxia* ('C-V'), but with a very short branch. This contrasts with the unconstrained analyses, where *Verreauxia* is sister to the remainder of *Goodenia* C (note asterisks at that node in Fig. 3). Within the remainder of *Goodenia* C, there are three additional clades that correspond, respectively, to 1) subsect. *Goodenia* ('C-G'); 2) subg. *Monochila* ('C-M'); and 3) subsect. *Scaevolina* ('C-S'). The latter two are sister to each other in most analyses, though with poor support (Fig. 3).

4. Discussion

4.1. Comparison of the results of CDS, NRR, and G3PDH datasets

Analyses of the CDS, NRR and G3PDH datasets generated in the current study largely corroborate the two-locus plastid phylogeny of Jabaily et al. (2012), but also achieve our primary goal of increasing backbone support. All branches but two receive maximum support in the CDS phylogeny (Fig. 1); this corroborates the results of many other recent studies that have used whole or nearly whole-plastome datasets to resolve phylogenies that had proved recalcitrant when only a few plastid loci were employed, including in Eucalypts (Bayly et al., 2013), commelinid monocots (Barrett et al., 2013), Zingiberales (Barrett et al., 2014), morning glories (Eserman et al., 2014), and Apocynaceae (Straub et al., 2014). The monophyly of *Scaevola* s.l., *Goodenia* s.l., *Coopernookia*, *Velleia* and clades B and C of *Goodenia* receive maximum or nearly maximum support in all analyses. A notable difference from Jabaily et al. (2012) is the well-supported placement of *Coopernookia* as sister to the remainder of *Goodenia* s.l. In the previous study, *Coopernookia* was placed as sister to *Goodenia* A with minimal support. The fully supported branch in our results that excludes *Coopernookia* from the remainder of *Goodenia* s.l. remains short in the CDS phylogeny, even with data from 70 genes, which may have contributed to the difficulty in resolving it in the earlier study.

While nearly all nodes in the CDS phylogeny received full support from all analyses (MP, ML, BI; Fig. 1), several relationships among the clades within *Goodenia* s.l. were less clearly resolved in the analyses based on nuclear G3PDH and NRR (Fig. 2). The NRR dataset recovers *Goodenia* A and B as sister clades, with low support, while the G3PDH dataset splits *Goodenia* A into a grade of two clades (A and A′, whose compositions mirror those found in *Goodenia* A via the other two datasets) subtending *Goodenia* B. Finally, MP analysis of the NRR dataset places *Velleia* sister to *Goodenia* B with weak support (not shown); ML and BI analyses of NRR recover the same relationship as the other datasets, with *Velleia* sister to *Goodenia* C with moderate support (Fig. 2). Conflicting results between the nuclear datasets and the CDS topology have much less support in the former than the latter. Other studies have also recovered generally lower support values in phylogenies based on nuclear datasets compared to plastid (e.g., Steele et al., 2012; Malé et al., 2014). The incongruence among the datasets is reflected in the results of pairwise partition homogeneity tests, in which the two nuclear-derived datasets are not significantly incongruent with one another, but both are significantly incongruent with the CDS (Fig. 2 and Supplementary Fig. S2). The results of the Shimodaira Approximately-Unbiased (AU) topology tests reflect the weak support in the NRR dataset, which did not statistically reject the CDS backbone topology of (*Goodenia* A (*Goodenia* B (*Velleia* + *Goodenia* C))). In contrast, the G3PDH dataset did statistically reject this topology. The plastome CDS alignment, which contained the most well-supported clades, significantly rejected the NRR and G3PDH backbone topology for *Goodenia* s.l. of ((*Goodenia* A + *Goodenia* B) (*Velleia* + *Goodenia* C)).

Incongruence between datasets was also found within *Goodenia* C, a clade that as currently circumscribed includes taxa from three genera (*Goodenia*, *Verreauxia*, and *Pentaptilon sensu* Jabaily et al., 2012) and considerable floral diversity (Fig. 1). The plastome CDS dataset yielded a topology of (C-C + (V + C-M)), whereas the G3PDH dataset yielded (C-M + (V + (C-C + C-S))), and the NRR dataset yielded (V + (C-C + C-M)) (Fig. 2 and Supplementary Fig. S2). All of these relationships receive strong support in their respective analyses (the lowest ML BS score at any of the relevant nodes is 92%); however, incomplete sampling of the subclades within *Goodenia* C between datasets reduces our ability to characterize these incongruences. The 98-taxon plastid dataset includes representatives of all five lineages within *Goodenia* C (Fig. 3), and the constrained and concatenated analyses of this dataset vary only in their placement of lineages at the base. The concatenated analyses recover (C-C + (V + (C-G + (C-M + C-S)))), while the unconstrained analyses reverse the positions of 'V' and 'C-C': (V + (C-C + (C-G + (C-M + C-S)))) (Fig. 3). All of these discordances between datasets reflect rapid diversification at the base of *Goodenia* C, perhaps accompanied by incomplete lineage sorting (ILS) or hybridization. Additional taxon sampling and sequence data from independent nuclear markers should shed more light on the interrelationships of these groups.

Several aspects of these datasets, especially the NRR, may affect the support inferred for *Goodenia* s.l. backbone relationships. These results illustrate the dramatic differences in inferred substitution rates between the sampled regions. In Core Goodeniaceae, the plastome CDS as a whole has evolved at roughly one-half the rate of G3PDH and one-fourth the rate of the NRR. Malé et al. (2014) found similarly higher substitution rates in NRR sequences assembled from genome skimming data, which they partially attributed to the generally higher rates of nuclear genome evolution in ribosomal DNA than in mitochondrial or plastid genomes (see also Wolfe et al., 1987). These rapid substitution rates may also cause incomplete concerted evolution in the NRR, leading to higher rates of polymorphic sites (Hillis et al., 1991). This may remove or obscure homologous characters and generate apparent homoplasy in the NRR, resulting in long terminal branch lengths and poor clade support deep in the phylogeny. This could also result in generally lower consistency and retention indices, which we see here (Fig. 2). Taken together, the high level of confidence we have in the CDS *Goodenia* s.l. phylogeny and the lower support levels from the nuclear data, especially the NRR, lead us to place greater confidence in the well-supported plastome-based topology for future taxonomic decisions. However, it is also possible that the discordance between nuclear and plastid histories may be the result of hybridization and/or polyploidy. This possibility deserves further investigation given the prevalence of these events in closely related Asteraceae (Barker et al., 2008), and interspecific variation in chromosome numbers reported within *Goodenia* s.l. and *Scaevola* s.l. (Peacock, 1963). Even if additional nuclear loci support a sister relationship between *Goodenia* A and *Goodenia* B, it is clear that the members of *Goodenia* B inherited a plastome more closely related to *Velleia* and *Goodenia* C than to the plastomes of *Goodenia* A. These plastome and NRR data represent a small portion (~3.5%) of the reads generated from the genome-skimming libraries, and we hope that additional assembly of slow-evolving COS markers (Mandel et al., 2014) and other nuclear loci will clarify the potential roles of hybridization or polyploidy in the diversification of Core Goodeniaceae.

4.2. Analyses of the 98-taxon plastid dataset and implications for taxonomy

Not surprisingly, enforcing a backbone topological constraint on the 98-taxon *trnL-trnF* and *matK* data matrix and concatenating the

CDS matrix to this dataset both resulted in stronger clade support values than in unconstrained analyses of the *trnL-trnF/matK* data (Fig. 3). The greatest improvement in support was at the node corresponding to *Goodenia* s.l., which received maximum support in the CDS (Fig. 1), constrained, and concatenated analyses, and moderate to low support (61/0.65/47 ML-BS/BI-PP/MP-BS) in the unconstrained analyses (Fig. 3). The high support for this particular node in the concatenated analyses, and resultant resolution of the relationship between *Goodenia* s.l. and *Coopernookia*, is a key result of the current work. Here, constraint and concatenation had nearly identical effects on results: both returned all of the major clades with nearly identical support values and topologies (Fig. 3). The nodes that received less than maximum statistical support resulted from placement of taxa that were not in the CDS matrix into different clades between analyses and bootstrap runs. In particular, we note that it is possible for constrained nodes to receive less than 100 support if the placement of additional taxa into these clades is inconsistent among bootstrap runs. One notable difference between the constrained and concatenated analyses is that, where the constrained analysis yielded short branches (i.e., between *Coopernookia* and *Goodenia* s.l., and between *Verreauxia* and *Goodenia* C clades C-G, C-M, and C-S), the concatenated analysis yielded longer branches (concatenated topology not shown). This is due to additional characters that support these branches in the concatenated dataset.

Outside of *Goodenia* s.l., *Brunonia*, *Scaevola*, and *Coopernookia* form a grade of mostly monophyletic genera (Fig. 3). *Brunonia* is a monotypic lineage on a very long branch that was previously placed in its own family (Carolin et al., 1992). *Scaevola* s.l. is sister to *Goodenia* s.l. plus *Coopernookia*, and (other than the inclusion of the monotypic genus *Diaspasis* and the exclusion of *Scaevola collaris*) the genus is monophyletic. However, its existing subgeneric taxonomy does not hold up, as the currently recognized sections are not resolved as monophyletic units in our phylogeny, corroborating previous results from Howarth et al. (2003) and Jabaily et al. (2012). *Scaevola* s.l. *in toto* is a clade of ca. 130 species that has radiated rapidly since only the mid Miocene (Jabaily et al., 2014), and methods that yield considerably more characters such as RADseq (Miller et al., 2007) or target-enrichment (Mandel et al., 2014) will be required to better characterize the relationships within *Scaevola* s.l. *Coopernookia* is consistently inferred to be a monophyletic genus sister to the remainder of *Goodenia* s.l. It is morphologically well characterized and is the only genus in the family with a base chromosome number of $x = 7$ (in *Brunonia australis* $x = 9$, and for all other genera in Core Goodeniaceae $x = 8$). *Coopernookia* was postulated to be sister to the remainder of Goodeniaceae (Carolin, 1978), and its monophyly is further supported by a unique suite of floral characters including the presence of flat hairs on the corolla wing margins and in the throat and glossy, strophiolate seeds (Carolin, 1968). Its position as recovered here, sister to the rest of *Goodenia* s.l. (Fig. 3), allows for the genus to be retained and will impact future character reconstruction efforts.

The clear paraphyly of *Goodenia* is the most pressing taxonomic concern. We recover three strongly supported clades within *Goodenia* (A, B, and C), one of which (C) is strongly supported as sister to *Velleia*, and contains a great deal of taxonomic diversity including smaller embedded genera (Fig. 3). In light of this topology, two options exist for naming monophyletic taxa within *Goodenia* s.l. The first includes expansion of the already large genus *Goodenia* (ca. 180 species) to include *Velleia* (ca. 21 species), *Verreauxia* (3 species), and monotypic *Selliera* and *Pentaptilon* (not included in the current study, but strongly supported as sister to *Verreauxia* in Jabaily et al., 2012). This would be congruent with other large molecular phylogenetic studies on Australian groups that resulted in proposed subsumation of genera (e.g., Orthia et al., 2005; Mast and Thiele, 2007; Shepherd and Wilson, 2007; Craven et al., 2014). The second option is the retention of at least some of the segregate genera and the elevation of some clades to generic status. We advocate the latter; the monophyly of *Velleia* has strong molecular and morphological support, and *Goodenia* has long been known to encompass substantial variation including a number of previously recognized genera. While there is some discordance among our datasets concerning the relationships of the major clades (Fig. 2), there is strong support for the monophyly of each, which will serve as the foundation for a new taxonomy currently underway by our group. Below we discuss several challenges to the existing classification of *Goodenia* presented by these phylogenies. Formal resolution of these issues awaits further sequencing of additional taxa not included in the current study and confirmation of synapomorphies that characterize monophyletic clades.

The *Goodenia* A clade encompasses considerable morphological and taxonomic variation (Fig. 1). It includes *G. ovata*, the type species of *Goodenia*, along with the majority of species in subsect. *Goodenia* characterized by bracteolate inflorescences and yellow, bilabiate flowers with hairs and enations inside the corolla. However, this clade also includes *G. phillipsiae*, a species noted to be of uncertain affinity by Carolin et al. (1992), which was included in subsect. *Ebracteolatae*. *Goodenia* A also includes *Scaevola collaris*, the monotypic genus *Selliera radicans*, and *G. viscida* (subg. *Monochila*), all of which possess fan-flowers (see Fig. 1 and below). The CDS and NRR datasets each recovered *Goodenia* A as monophyletic with strong support, while G3PDH split *Goodenia* A into two clades, one of which (A′) is sister to *Goodenia* B, but with very low support (Fig. 2). We are inclined to follow the plastome and NRR topologies, but data from additional nuclear markers and increased taxon sampling will help to clarify whether *Goodenia* A′ is more closely related to *Goodenia* B or *Goodenia* A.

Goodenia B is largely composed of members of subsect. *Ebracteolatae*, which generally comprise ebracteolate plants with articulated pedicels. This clade has a basal grade that includes members of sects. *Porphyranthus* and *Amphichila*. The former includes yellow and purple flowered species, of which *G. lamprosperma* F. Muell., *G. nocoleche* Pellow & J. L. Porter and *G. berringbinensis* Carolin have been recorded growing in seasonally wet habitats and may exhibit an aquatic stage (Pellow and Porter, 2005; Gibson, 2014). *Goodenia pumilo* R. Br and *G. kakadu* Carolin are small, red–purple flowered, short-lived herbs from northern Australia also confined to seasonally wet habitats and are the only taxa currently included in sect. *Amphichila.* The *Goodenia* B clade also includes one member of subsect. *Goodenia* (*G. wilunensis* Carolin), and several members of subsect. *Borealis.* Further investigation is required to determine if these taxa possess cohesive morphological features that could support relationships previously overlooked.

Velleia is strongly supported as the sister clade to *Goodenia* C in all analyses (Fig. 2). Within *Velleia*, sect. *Menoceras* appears to be paraphyletic, with at least one embedded member of sect. *Euthales* (*V. foliosa* (Benth.) K. Krause) (Fig. 3). However, the genus as a whole is well-supported as distinct from other members of the family by morphological characters along with our molecular data (Carolin et al., 1992; Jabaily et al., 2012).

Goodenia C is composed of five well-supported clades (Fig. 3), and while the order of divergence among these varies among our datasets (Fig. 2), none of the conflicting topologies will impact taxonomic outcomes as the individual clades comprise discrete infrageneric groups or long recognized genera. For example, *Verreauxia* and *Pentaptilon* ('V'), described by Bentham and Pritzel in 1868 and 1905, respectively, are characterized by the presence of distinctive multicellular hairs and nut-like fruits, which are uniquely winged in *Pentaptilon.* The members of subsect. *Coeruleae* ('C-C') occur in southwestern Australia and include blue, bilabiate-flowered species with seeds that have a narrow, mucilaginous wing ca. 0.1 mm wide. Similarly, the members of subsect. *Scaevolina*

('C-S') also have blue, bilabiate- or fan-flowers, but are predominantly from northern Australia and have seeds with a wing > 0.1 mm wide. Members of subg. *Monochila* ('C-M') have white or cream fan-flowers with purplish spots in the throat, and an oblong indusium. The only exception is the yellow-flowered *G. viscida*, which was previously included in subg. *Monochila* largely based on its fan-flower morphology (Carolin et al., 1992) but is now shown to be allied to members of *Goodenia* A. The final clade recovered within *Goodenia* C includes members of subsect. *Goodenia* ('C-G') that are predominantly from eastern Australia and have paniculate inflorescences, yellow flowers that often have cottony hairs on the outer surface and erect-connivent, adaxial lobes, and reticulate-pitted seeds. While further investigation is required to identify consistent synapomorphies for each of these groups, it is evident from our analyses that they represent distinct clades and are likely to warrant recognition as segregate genera.

4.3. Floral symmetry evolution

A fully resolved phylogeny of the Core Goodeniaceae has major implications for reconstruction of morphological characters in a comparative framework. Of particular interest are petal symmetry shifts that appear to be frequent within this clade but rare in its sister clade, which consists of nearly uniformly bilabiate-flowered species of *Lechenaultia*, *Anthotium*, and *Dampiera* (Jabaily et al., 2012). The fan-flower symmetry, with all five petals positioned on the dorsal side of the corolla tube slit (Fig. 1), is most likely a convergent morphology that has led to the incorrect assumption of relatedness among non-monophyletic taxa. For example, fan-flowers are found in all of *Scaevola* s.l. except for monotypic *Diaspasis*, which has nearly actinomorphic flowers. This morphology has also evolved independently at least three times in *Goodenia* (Fig. 1): white, fan-flowered members of subg. *Monochila* s.s. are sister to clades of species with yellow or blue bilabiate flowers in *Goodenia* C, while fan-flowers may have evolved twice in *Goodenia* clade A along the branches leading to *G. viscida*, and *Scaevola collaris* plus *Selliera radicans*. In addition, interpreting the symmetry of monotypic *Brunonia australis* (sister to the remainder of the Core Goodeniaceae) is complicated by the fact that it is the lone taxon in Goodeniaceae that does not possess a slit of the corolla tube, and thus it has been described as the only truly actinomorphic member of the family (Carolin, 1978). Its flowers are condensed into crowded, head-like inflorescences, and the free distal portions of the petals in these small flowers tend to be on one side like a fan-flower. Reconstructing floral symmetry evolution across the phylogeny of Core Goodeniaceae will depend on the interpretation of homology, which is informed by phylogeny and developmental studies. Further analysis of floral form evolution currently underway by our group will include a systematically-informed, geometric-morphometric approach to identify floral symmetry categories, paired with analyses of petal-specific expression data.

4.4. Conclusion

The investment in NGS for this project has yielded a fully resolved plastome phylogeny for the Core Goodeniaceae, much of which is corroborated by nuclear genetic histories. The plastome CDS includes a large amount of sequence data that evolved at a relatively conserved rate, yielding a completed resolved and very strongly supported phylogeny. Though this backbone topology continues to have very short branches compared to the tip-ward relationships among taxa seen in the 98-taxon analyses, phylogenetic support is maximal in almost all cases. The nuclear G3PDH and NRR datasets largely corroborate this topology, though they suggest slightly different (though less well-supported) relationships among clades within *Goodenia* s.l. Future analyses will focus on including additional nuclear genomic data, to further explore these relationships and to ascertain the potential roles of hybridization, polyploidy, and/or incomplete lineage sorting. These phylogenetic inferences make clear that several taxonomic changes are needed within Core Goodeniaceae. These include generic transfers for some enigmatic species possessing atypical floral symmetries (*Scaevola collaris*, *Selliera radicans*, and *Diaspasis filifolia*), along with the potential splitting of *Goodenia* s.l. into as many as seven segregate genera corresponding with *Goodenia* A, *Goodenia* B, and five clades within *Goodenia* C. We are re-examining these taxa in light of our findings to identify morphological synapomorphies in support of these phylogenetic relationships. In addition to taxonomic changes, we highlight the striking floral diversity among the Core Goodeniaceae. Among many other shifts, fan-flowers appear to have evolved repeatedly, though the level of homology among these transitions remains unclear.

Acknowledgments

The authors thank the following people and institutions for providing field and laboratory support, tissue samples, and comments on the manuscript: Spencer Willis, Leigh Sage, Juliet Wege, Carol Wilkins, Andrew Perkins, Bob and Shona Chinnock, Digby Growns and Kings Park Botanic Gardens, Vanessa Westcott and Luke Bayley from Bush Heritage Australia, herbaria PERTH, DNA, AD, CANB, MEL and NSW, J. Chris Pires, several anonymous reviewers, and the University of Florida Phylogenetic Systematics Seminar Series. Funding for this study was provided by the National Science Foundation (NSF DEB 1256946 to RSJ, DGH).

Appendix A

Voucher and GenBank information for the accessions used in this study: Information is comma-delimited in this order: Taxon, Collector, Collector number, GenBank accession numbers for DNA sequences listed in order of *matK*, *trnL-trnF*, *G3PDH*, Plastome CDS, Nuclear Ribosomal Repeat (see Tables A and B).

Brunonia australis R.Br., *K.A. Shepherd*, *KS1512*, *KT724262*, *KT750314*, –, *KT750327*, *KR264952*; *Coopernookia georgei Carolin*, *M. Crowhurst*, *25A*, –, –, *KP689358*, –, –; *Coopernookia polygalacea (de Vriese) Carolin*, *K.A. Shepherd*, *KS1521*, *KT724237*, *KT750273*, *KP689378*, *KP828778*, *KR604962*; *Coopernookia strophiolata (F. Muell.) Carolin*, *K.A. Shepherd*, *KS1534*, *KT724265*, *KT750320*, *KP689352*, *KP828785*, *KR604963*; *Diaspasis filifolia R.Br.*, *K.A. Shepherd*, *KS1520*, *KT724266*, *KT750317*, *KP689361*, *KP828798*, *KR604955*; *Goodenia aff. grandiflora Sims*, *M. Parris*, *9695*,

Table A
Infrageneric classification of the genus *Goodenia* following Carolin et al., 1992.

Subgenus	Section	Subsection	Series
Goodenia Sm.	***Amphichila*** DC.		
	Coeruleae (Benth.) Carolin	***Coeruleae*** (Benth.) ***Carolin***	
		Scaevolina Carolin	
	Goodenia Sm.	***Borealis*** Carolin	***Borealis*** Carolin
			Calogyne (R.Br.) Carolin
		Ebracteolatae K. Krause	
		Goodenia Sm.	
	Porphyranthus G.Don.		
Monochila (G. Don) Carolin			

Table B
Total reads, number of reads aligned to *Helianthus annuus* plastome, total plastome assembly length, length of CDS only, average coverage of plastome, number of reads aligned to *H. annuus* nuclear ribosomal repeat (NRR), total NRR assembly length (>25×) and average coverage of NRR for 24 Core Goodeniaceae and *H. annuus* reference sequences (NC_007977 and KF767534).

Species	Total reads	No. reads aligned to *H. annuus* plastome	Total plastome assembly length	Length of CDS only	Average coverage of plastome	No. reads aligned to *H. annus* NRR	Total NRR assembly length (>25×)	Average coverage of NRR
Helianthus annuus	–	–	126,471*	84,209	–	–	9814	–
Brunonia australis	20,298,026	253,632	135,642	39,070	310	509,262	6967	79,117
Coopernookia polygalacea	15,686,920	359,072	136,918	50,522	433	107,949	6966	2029
Coopernookia strophiolata	18,376,278	227,461	135,029	50,523	274	100,087	7635	1931
Diaspasis filifolia	17,147,606	836,333	141,399	51,512	1012	124,158	7527	2607
Goodenia decursiva	22,847,200	532,701	140,674	50,584	646	322,838	7836	12,400
Goodenia drummondii	20,031,232	537,658	140,925	50,546	655	483,065	7579	11,123
Goodenia filiformis	19,923,330	413,931	139,777	43,154	517	203,625	6951	3180
Goodenia hassallii	19,548,116	829,815	143,815	50,548	1013	208,368	7147	5294
Goodenia helmsii	19,313,898	361,406	137,631	50,560	440	382,087	7505	5573
Goodenia micrantha	16,788,718	541,667	137,301	43,285	666	529,026	7126	12,261
Goodenia ovata	20,482,178	400,595	137,614	50,558	486	368,936	7380	17,053
Goodenia phillipsiae	24,145,646	610,353	139,327	50,522	741	88,090	6833	1952
Goodenia pinifolia	20,806,614	1,240,958	144,878	50,544	1529	107,690	7954	4175
Goodenia tripartita	18,400,166	325,856	136,934	50,229	403	436,635	7858	16,216
Goodenia viscida	17,499,710	293,136	136,364	51,005	354	105,909	7476	2316
Scaevola collaris	20,480,206	671,299	139,441	50,997	812	101,477	7237	2392
Scaevola porocarya	14,830,644	368,182	138,325	52,336	443	167,735	7411	3086
Scaevola phlebopetala	22,302,836	307,138	138,951	51,272	370	248,477	7834	7971
Scaevola tomentosa	19,294,312	764,585	142,842	51,870	923	170,155	7627	3843
Selliera radicans	20,691,984	509,469	137,610	50,506	624	42,395	7076	849
Velleia discophora	16,425,972	184,544	135,223	50,911	228	452,092	7107	9269
Velleia foliosa	19,506,716	1,582,864	146,350	50,437	1967	325,881	7656	14,004
Velleia rosea	16,823,610	690,027	139,151	45,492	865	406,818	7166	19,063
Verreauxia reinwardtii	21,007,648	765,972	142,932	49,427	933	196,188	7180	2895

* Length of *H. annuus* plastome after one copy of the inverted repeat is removed; total length of NC_007977 is 151,104.

JQ711633, *JQ682740*, –, –, –; *Goodenia angustifolia Carolin*, *P. Latz & A. Schubert*, *26410*, *KT724216*, *KT750319*, –, –, –; *Goodenia atriplexifolia A.E. Holland & T.P. Boyle*, *A.R. Bean*, *22440*, *KT724229*, *KT750270*, –, –, –; *Goodenia azurea F. Muell.*, *P.A. Fryxell*, *L.A. Craven*, *J. McD. Stewart*, *4485*, *KT724222*, *KT750280*, *KP689357*, –, –; *Goodenia bellidifolia Sm. subsp. bellidifolia*, *Robinson* et al., *86-0235*, *JQ711594*, *JQ682833*, –, –, –; *Goodenia benthamiana Carolin*, *J. Connock*, *395*, *KT724278*, *KT750286*, –, –, –; *Goodenia campestris Carolin*, *R.M. Barker*, *222*, *JQ711608*, *JQ682815*, –, –, –; *Goodenia claytoniacea Benth.*, *F. Hort*, *2135*, –, –, *KP689379*, –, –; *Goodenia convexa Carolin*, *B.H. Smith*, *777*, *JQ711613*, *JQ682658*, –, –, –; *Goodenia coronopifolia R. Br.*, *J. Egan*, *4378*, *JQ711627*, *JQ682854*, –, –, –; *Goodenia corynocarpa F. Muell.*, *G. Byrne*, *2408*, –, –, *KP689377*, –, –; *Goodenia decurrens R. Br.*, *F.E. Davies*, *346*, *JQ711689*, *JQ682788*, –, –, –; *Goodenia decursiva W. Fitzg.*, *K.A. Shepherd*, *KS1528*, *KT724263*, *KT750302*, *KP689374*, *KP828786*, *KR604958*; *Goodenia dimorpha Maiden & Betche*, *F.E. Davies*, *323*, *JQ711610*, *JQ682800*, –, –, –; *Goodenia disperma F. Muell.*, *B.J. Lepschi*, *1164*, *JQ711569*, *JQ682792*, –, –, –; *Goodenia drummondii Carolin*, *K.A. Shepherd*, *KS1516*, *KT724248*, *KT750271*, *KP689363*, *KP828776*, *KR604951*; *Goodenia eatoniana F. Muell.*, *B. Barnsley*, *776*, *JQ711570*, *JQ682821*, –, –, –; *Goodenia elongata Labill.*, *I. Crawford*, *7038*, *JQ711652*, *JQ682654*, –, –, –; *Goodenia eremophila E. Pritz.*, *J. Taylor*, *495*, *JQ711695*, *JQ682834*, –, –, –; *Goodenia fasciculatis F. Muell. & Tate*, *N.N. Donner*, *6686*, *JQ711587*, *JQ682723*, *KP689351*, –, –; *Goodenia fasciculata (Benth.) Carolin*, *R. Hamilton*, *67*, *JQ711686*, *JQ682750*, –, –, –; *Goodenia faucium Carolin*, *P.K. Latz*, *7521*, *JQ711693*, *JQ682689*, –, –, –; *Goodenia filiformis R.Br.*, *K.A. Shepherd*, *KS1529*, *KT724267*, *KT750316*, –, *KP828779*, *KR604956*; *Goodenia fordiana Carolin*, *P. Gilmour*, *7360*, *JQ711648*, *JQ682739*, –, –, –; *Goodenia glabra R.Br.*, *E.M. Canning*, *5822*, *JQ711577*, *JQ682829*, –, –, –; *Goodenia glauca F. Muell.*, *T.R. Lally*, *325*, *JQ711682*, *JQ682738*, *KP689349*, –, –; *Goodenia glomerata Maiden & Betche*, *J. McAuliffe*, *190*, *JQ711691*, *JQ682826*, –, –, –; *Goodenia goodeniacea (F. Muell.) Carolin*, *B. J. Lepschi*, *4808*, *JQ711694*, *JQ682718*, –, –, –; *Goodenia granitica L.W. Sage & K.A. Sheph.*, *B. Lullfitz*, *BRL 074*, –, –, *KP689367*, –, –; *Goodenia gypsicola Symon*, *S. van Leeuwen*, *4957*, –, –, *KP689365*, –, –; *Goodenia hartiana L.W. Sage*, *S. Santich*, *s.n.*, –, –, *KP689359*, –, –; *Goodenia hassallii F. Muell.*, *K.A. Shepherd*, *KS1517*, *KT724268*, *KT750288*, *KP689380*, *KP828783*, *KR604947*; *Goodenia havilandii Maiden & Betche*, *Greuter*, *s.n.*, *KT724250*, *KT750306*, *KP689364*, –, –; *Goodenia helmsii (E. Pritz.) Carolin*, *K.A. Shepherd*, *KS1511*, *KT724243*, *KT750321*, –, *KP828780*, *KR604945*; *Goodenia iyouta Carolin*, *P.K. Latz*, *17843*, *KT724256*, *KT750285*, –, –, –; *Goodenia janamba Carolin*, *D.L. Lewis*, *1341*, *KT724254*, *KT750292*, *KP689366*, –, –; *Goodenia lamprosperma F. Muell.*, *K. Brennan*, *9561*, *KT724273*, *KT750289*, –, –, –; *Goodenia lineata J.H. Willis*, *J.A. Jeanes*, *G. Lay*, *2286*, *KT724215*, *KT750283*, –, –, –; *Goodenia macroplectra (F. Muell.) Carolin*, *R.J. Cranfield*, *7667*, *JQ711576*, *JQ682696*, –, –, –; *Goodenia micrantha Hemsl. ex Carolin*, *K.A. Shepherd*, *KS1510*, *KT724228*, *KT750262*, –, *KP828796*, *KR604960*; *Goodenia microptera F. Muell.*, *A.A. Mitchell*, *PRP516*, *JQ711663*, *JQ682732*, –, –, –; *Goodenia nigrescens Carolin*, *C.R. Michell*, *R.B. Carrow*, *1323*, *KT724214*, *KT750293*, *KP689354*, –, –; *Goodenia nuda E. Pritz.*, *A.A. Mitchell*, *PRP 547*, *JQ711696*, *JQ682710*, –, –, –; *Goodenia ovata Sm.*, *K.A. Shepherd*, *KS1530*, *KT724275*, *KT750309*, *KP689373*, *KP828784*, *KR604946*; *Goodenia phillipsiae Carolin*, *K.A. Shepherd*, *KS1527*, *KT724238*, *KT750308*, –, *KP828791*, *KR604965*; *Goodenia pinifolia de Vriese*, *K.A. Shepherd*, *KS1532*, *KT724235*, *KT750282*, *KP689376*, *KP828792*, *KR604948*; *Goodenia pinnatifida Schltdl.*, *E. Brown*, *28.9.1978*, *KT724269*, *KT750323*, –, –, –; *Goodenia prostrata Carolin*, *R. Chinnock*, *S. Chinnock*, *RJC 10292*, *KT724258*, *KT750313*, –, –, –; *Goodenia pulchella Benth.*, *J.E. Wajon*, *1246*, *KT724261*, *KT750287*, –, –, –; *Goodenia decurrens R.Br.*, *D.L. Lewis*, *J. Harding*, *2127*, *KT724224*, *KT750324*, –, –, –; *Goodenia purpurascens R.Br.*, *D. Napier*, *314*, *KT724233*, *KT750297*, –, –, –; *Goodenia purpurea (F. Muell.) Carolin*, *P.C. Jobson*, *1356*, *KT724271*,

KT750274, –, –, –; *Goodenia pusilliflora F. Muell.*, *D.E. Symon*, *4292*, *JQ711635*, *JQ682751*, –, –, –; *Goodenia quasilibera Carolin*, *D.J. Edinger* et al., *DJE 2972*, *KT724245*, *KT750303*, –, –, –; *Goodenia racemosa F. Muell. var. racemosa*, *A.R. Bean*, *8957*, *KT724231*, *KT750322*, –, –, –; *Goodenia ramelii F. Muell.*, *K. Brennan*, *9564*, *KT724246*, *KT750312*, *KP689350*, –, –; *Goodenia redacta Carolin*, *I.D. Cowie*, *J. Palmer*, *13476*, *KT724239*, *KT750295*, –, –, –; *Goodenia robusta (Benth.) K. Krause*, *Hj. Eichler*, *14037*, *JQ711620*, *JQ682661*, *KP689368*, –, –; *Goodenia rosulata Domin*, *A.R. Bean*, *18304*, *KT724244*, *KT750299*, –, –, –; *Goodenia saccata Carolin*, *Badman*, *5148*, *KT724257*, *KT750265*, –, –, –; *Goodenia scaevolina F. Muell.*, *K.G. Brennan*, *T.A. Calnan*, *7382*, –, –, *KP689360*, –, –; *Goodenia scapigera subsp. granitica L.W. Sage*, *J.A. Cochrane*, *B. Davis*, *JAC 6911*, *KT724264*, *KT750279*, –, –, –; *Goodenia sepalosa Benth.*, *P.A. Fryxell*, *L.A. Craven*, *J. McD. Stewart*, *4195*, *KT724226*, *KT750305*, –, –, –; *Goodenia splendida A.E. Holland & T.P. Boyle*, *K.R. McDonald*, *KRM452*, *KT724247*, *KT750275*, –, –, –; *Goodenia stelligera R.Br.*, *P.I. Forster*, *PIF 29042*, *KT724232*, *KT750266*, –, –, –; *Goodenia stephensonii F. Muell.*, *Cassis*, *Schuh*, *& Schwartz*, *s.n.*, *KT724255*, *KT750300*, –, –, –; *Goodenia stirlingii F.M. Bailey*, *P.I. Forster*, *K.R. McDonald*, *R. Jenzen*, *PIF 30928*, *KT724280*, *KT750278*, –, –, –; *Goodenia stobbsiana F. Muell.*, *B. Chinnock*, *S. Chinnock*, *RJC 10301*, *KT724241*, *KT750272*, –, –, –; *Goodenia strangfordii F. Muell.*, *K. Brennan*, *8545*, *KT724276*, *KT750284*, –, –, –; *Goodenia tenuiloba F. Muell.*, *B. Chinnock*, *S. Chinnock*, *RJC 10312*, *KT724242*, *KT750264*, –, –, –; *Goodenia tripartita Carolin*, *K.A. Shepherd*, *KS1524*, *KT724270*, *KT750259*, *KP689362*, *KP828777*, *KR604954*; *Goodenia varia R.Br.*, *D.J.E. Whibley*, *1645*, *JQ711562*, *JQ682762*, –, –, –; *Goodenia viscida R.Br.*, *K.A. Shepherd*, *KS1536*, *KT724279*, *KT750326*, *KP689371*, *KP828797*, *KR604949*; *Goodenia wilunensis Carolin*, *R. Meissner*, *B. Bayliss*, *895*, *KT724249*, *KT750294*, –, –, –; *Scaevola amblyanthera F. Muell. var. centralis Carolin*, *R. Davis*, *J. Jackson*, *G. Hearle*, *11704*, *KT724234*, *KT750296*, –, –, –; *Scaevola browniana Carolin subsp. browniana*, *R. Booth*, *D.T. Kelman*, *5379*, *KT724240*, *KT750304*, –, –, –; *Scaevola bursariifolia J.M. Black*, *D.E. Symon*, *4580*, *JQ711656*, *JQ682666*, –, –, –; *Scaevola canescens Benth.*, *R. Davis*, *RD 11752*, *KT724225*, *KT750263*, *KP689348*, –, –; *Scaevola collaris J.M. Black ex E.L. Robertson*, *K.A. Shepherd*, *KS1533*, *KT724251*, *KT750298*, –, *KP828787*, *KR604959*; *Scaevola enantophylla F. Muell.*, *P.I. Forster*, *R. Booth*, *R. Jensen*, *PIF 27552*, *KT724230*, *KT750276*, –, –, –; *Scaevola gaudichaudii Hook. & Arn.*, *D. Howarth*, *32*, –, –, *AY894491*, –, –; *Scaevola kilaueae O. Deg.*, *Morden*, *1141*, –, –, *AY894493*, –, –; *Scaevola oldfieldii F. Muell.*, *A. Crawford*, *ADC 863*, *KT724277*, *KT750307*, –, –, –; *Scaevola ovalifolia R.Br.*, *T.R.N. Lothian*, *3294*, *JQ711580*, *JQ682824*, –, –, –; *Scaevola phlebopetala F. Muell.*, *K.A. Shepherd*, *KS1519*, *KT724260*, *KT750301*, –, *KP828782*, *KR604957*; *Scaevola platyphylla Lindl.*, *K.A. Shepherd*, *J. Wege*, *KS 926*, *KT724220*, *KT750315*, –, –, –; *Scaevola porocarya F. Muell.*, *K.A. Shepherd*, *KS1518*, *KT724236*, *KT750260*, –, *KP828794*, *KR604961*; *Scaevola repens de Vriese*, *M. Gustafsson & K. Bremer*, *113*, *JQ711670*, *JQ682807*, –, –, –; *Scaevola sericophylla F. Muell. ex Benth.*, *R. Davis*, *RD14753*, *KT724281*, *KT750291*, –, –, –; *Scaevola spinescens R.Br.*, *A.R. Bean*, *29501*, *KT724221*, *KT750310*, –, –, –; *Scaevola subcapitata F.Br.*, *Lorence*, *8167*, *JQ711622*, *JQ682704*, –, –, –; *Scaevola taccada (Gaertn.) Roxb.*, *Beach*, *s.n.*, *KT724218*, *JQ682857*, –, –, –; *Scaevola thesioides Benth. subsp. filifolia (E. Pritz.) Carolin*, *K.A. Shepherd*, *C. Wilkins*, *J.A. Wege*, *KS1488*, *KT724272*, *KT750318*, *KP689356*, –, –; *Scaevola tomentosa Gaudich.*, *K.A. Shepherd*, *KS1523*, *KT724253*, *KT750268*, *KP689370*, *KP828789*, *KR604953*; *Selliera radicans Cav.*, *K.A. Shepherd*, *KS1535*, *KT724259*, *KT750261*, –, *KP828795*, *KR604943*; *Velleia connata F. Muell.*, *R. Davis*, *J. Jackson*, *D. Ferguson*, *11635*, *KT724217*, *KT750290*, *KP689355*, –, –; *Velleia discophora F. Muell.*, *K.A. Shepherd*, *KS1513*, *KT724223*, *KT750277*, *KP689353*, *KP828790*, *KR604950*; *Velleia foliosa (Benth.) K. Krause*, *K.A. Shepherd*, *KS1526*, *KT724252*, *KT750281*, –, *KP828788*, *KR604952*; *Velleia macrocalyx Vriese*, *P.K. Latz*, *19355*, –, –, *KP689369*, –, –; *Velleia glabrata Carolin*, *R. Davis*, *J. Jackson*, *11537*, *KT724227*, *KT750325*, –, –, –; *Velleia rosea S. Moore*, *K.A. Shepherd*, *KS1509*, *KT724219*, *KT750311*, *KP689375*, *KP828793*, *KR604944*; *Verreauxia reinwardtii (de Vriese) Beth.*, *K.A. Shepherd*, *KS1514*, *KT724274*, *KT750269*, –, *KP828781*, *KR604964*; *Verreauxia reinwardtii (de Vriese) Beth.*, *G.J. Keighery*, *16861*, –, –, *KP689372*, –, –.

Appendix B. Supplementary material

Supplementary data associated with this article can be found, in the online version, at http://dx.doi.org/10.1016/j.ympev.2015.10.003.

References

Altekar, G., Dwarkadas, S., Huelsenbeck, J.P., Ronquist, F., 2004. Parallel metropolis coupled Markov chain Monte Carlo for Bayesian phylogenetic inference. Bioinformatics 20, 407–415.

Barker, M.S., Kane, N.C., Matvienko, M., Kozik, A., Michelmore, R.W., Knapp, S.J., Rieseberg, L.H., 2008. Multiple paleopolyploidizations during the evolution of the Compositae reveal parallel patterns of duplicate gene retention after millions of years. Mol. Biol. Evol. 25, 2445–2455.

Barrett, C.F., Davis, J.I., Leebens-Mack, J., Conran, J.G., Stevenson, D.W., 2013. Plastid genomes and deep relationships among the commelinid monocot angiosperms. Cladistics 29, 65–87.

Barrett, C.F., Specht, C.D., Leebens-Mack, J., Stevenson, D.W., Zomlefer, W.B., Davis, J. I., 2014. Resolving ancient radiations: can complete plastid gene sets elucidate deep relationships among the tropical gingers (Zingiberales)? Ann. Bot. 113, 119–133.

Bayly, M.J., Rigault, P., Spokevicius, A., Ladiges, P.Y., Ades, P.K., Anderson, C., Bossinger, G., et al., 2013. Chloroplast genome analysis of Australian eucalypts – Eucalyptus, Corymbia, Angophora, Allosyncarpia and Stockwellia (Myrtaceae). Mol. Phylogenet. Evol. 69, 704–716.

Bock, D.G., Kane, N.C., Ebert, D.P., Rieseberg, L.H., 2014. Genome skimming reveals the origin of the Jerusalem Artichoke tuber crop species: neither from Jerusalem nor an artichoke. New Phytol. 201, 1021–1030.

Carolin, R.C., 1968. *Coopernookia*: a new genus of Goodeniaceae. Proc. Linnean Soc. NSW 92, 209–216.

Carolin, R.C., 1978. The systematic relationships of *Brunonia*. Brunonia 1, 9–29.

Carolin, R.C., Rajput, M.T.M., Morrison, P., 1992. Goodeniaceae. In: George, A.S. (Ed.), Flora of Australia volume 35. Australian Government Publishing Service, Canberra, pp. 4–300.

Cho, S., Zwick, A., Regier, J.C., Mitter, C., Cummings, M.P., Yao, J., Du, Z., et al., 2011. Can deliberately incomplete gene sample augmentation improve a phylogeny estimate for the advanced moths and butterflies (Hexapoda: Lepidoptera)? Syst. Biol. 60, 782–796.

Craven, L.A., Edwards, R.D., Cowley, K.J., 2014. New combinations and names in *Melaleuca* (Myrtaceae). Taxon 63, 663–670.

Darriba, D., Taboada, G.L., Doallo, R., Posada, D., 2012. JModelTest 2: more models, new heuristics and parallel computing. Nat. Methods 9, 772-772.

Davis, J.I., McNeal, J.R., Barrett, C.F., Chase, M.W., Cohen, J.I., Duvall, M.R., Givnish, T. J., et al., 2013. Contrasting patterns of support among plastid genes and genomes for major clades of the monocotyledons. In: Wilkin, P., Mayo, S.J. (Eds.), Early Events in Monocot Evolution. Cambridge University Press, pp. 315–349.

Drummond, A.J., Rambaut, A., 2007. BEAST: Bayesian evolutionary analysis by sampling trees. BMC Evol. Biol. 7, 214–222.

Drummond, A.J., Suchard, M.A., Xie, D., Rambaut, A., 2012. Bayesian phylogenetics with BEAUti and the BEAST 1.7. Mol. Biol. Evol. 29, 1969–1973.

Edgar, R.C., 2004. MUSCLE: multiple sequence alignment with high accuracy and high throughput. Nucleic Acids Res. 32, 1792–1797.

Eserman, L.A., Tiley, G.P., Jarret, R.L., Leebens-Mack, J.H., Miller, R.E., 2014. Phylogenetics and diversification of morning glories (tribe Ipomoeeae, Convolvulaceae) based on whole plastome sequences. Am. J. Bot. 101, 92–103.

Farris, J.S., Källersjö, M., Kluge, A.G., Bult, C., 1994. Testing the significance of incongruence. Cladistics 10, 315–319.

Gibson, N., 2014. An amphibious *Goodenia* (Goodeniaceae) from an ephemeral arid zone wetland. Nuytsia 24, 23–28.

Givnish, T.J., Ames, M., McNeal, J.R., McKain, M.R., Steele, P.R., dePamphilis, C.W., Graham, S.W., et al., 2010. Assembling the tree of the monocotyledons: plastome sequence phylogeny and evolution of Poales. Ann. Mo. Bot. Gard. 97, 584–616.

Hillis, D.M., Moritz, C., Porter, C.A., Baker, R.J., 1991. Evidence for biased gene conversion in concerted evolution of ribosomal DNA. Science 251, 308–310.

Howarth, D.G., Gustafsson, M.H.G., Baum, D.A., Motley, T.J., 2003. Phylogenetics of the genus *Scaevola* (Goodeniaceae): implications for dispersal patterns across the Pacific Basin and colonization of the Hawaiian Islands. Am. J. Bot. 90, 915–923.

Howarth, D.G., Baum, D.A., 2005. Genealogical evidence of homoploid hybrid speciation in an adaptive radiation of *Scaevola* (Goodeniaceae) in the Hawaiian Islands. Evolution 59, 948–961.

Jabaily, R.S., Shepherd, K.A., Gustafsson, M.H.G., Sage, L.W., Krauss, S.L., Howarth, D. G., Motley, T.J., 2012. Systematics of the Austral-Pacific family Goodeniaceae: establishing a taxonomic and evolutionary framework. Taxon 61, 419–436.

Jabaily, R.S., Shepherd, K.A., Gardner, A.G., Gustafsson, M.H.G., Howarth, D.G., Motley, T.J., 2014. Historical biogeography of the predominantly Australian plant family Goodeniaceae. J. Biogeogr. 41, 2057–2067.

Jian, S., Soltis, P.S., Gitzendanner, M.A., Moore, M.J., Li, R., Hendry, T.A., Qiu, Y.-L., et al., 2008. Resolving an ancient, rapid radiation in Saxifragales. Syst. Biol. 57, 38–57.

Katoh, K., Standley, D.M., 2013. MAFFT multiple sequence alignment software version 7: improvements in performance and usability. Mol. Biol. Evol. 30, 772–780.

Leaché, A.D., Wagner, P., Linkem, C.W., Böhme, W., Papenfuss, T.J., Chong, R.A., Lavin, B.R., et al., 2014. A hybrid phylogenetic–phylogenomic approach for species tree estimation in African *Agama* lizards with applications to biogeography, character evolution, and diversification. Mol. Phylogenet. Evol. 79, 215–230.

Ma, P.F., Zhang, Y.X., Zeng, C.X., Guo, Z.H., Li, D.Z., 2014. Chloroplast Phylogenomic Analyses Resolve Deep-Level Relationships of an Intractable Bamboo Tribe Arundinarieae (Poaceae). System. Biol., First published online August 4, 2014. doi: 10.1093/sysbio/syu054.

Malé, P.J.G., Bardon, L., Besnard, G., Coissac, E., Delsuc, F., Engel, J., Lhuillier, E., et al., 2014. Genome skimming by shotgun sequencing helps resolve the phylogeny of a pantropical tree family. Molecul. Ecol. Resour. 14, 966–975.

Mandel, J.R., Dikow, R.B., Funk, V.A., Masalia, R.R., Staton, S.E., Kozik, A., Michelmore, R.W., et al., 2014. A target enrichment method for gathering phylogenetic information from hundreds of loci: an example from the Compositae. Appl. Plant Sci. 2, 1300085.

Mast, A.R., Thiele, K.T., 2007. The transfer of *Dryandra* R.Br. to *Banksia* L.F. (Proteaceae). Aust. Syst. Bot. 20, 63–71.

Miller, M.R., Dunham, J.P., Amores, A., Cresko, W.A., Johnson, E.A., 2007. Rapid and cost-effective polymorphism identification and genotyping using restriction site associated DNA (RAD) markers. Genome Res. 17, 240–248.

Moore, M.J., Soltis, P.S., Bell, C.D., Burleigh, J.G., Soltis, D.E., 2010. Phylogenetic analysis of 83 plastid genes further resolves the early diversification of eudicots. Proc. Nation. Acad. Sci. USA 107, 4623–4628.

Orthia, L.A., Crisp, M.D., Cook, L.G., Kok, de R.P.J., 2005. Bush peas: a rapid radiation with no support for monophyly of Pultenaea (Fabaceae: Mirbelieae). Aust. Syst. Bot. 18, 133–147.

Peacock, W.J., 1963. Chromosome numbers and cytoevolution in the Goodeniaceae. Proc. Linnean Soc. NSW 88, 8–27.

Pellow, B.J., Porter, J.L., 2005. A new species of *Goodenia* (Goodeniaceae) from Nocoleche Nature Reserve, Far Western Plains, New South Wales. Telopea 11, 31–41.

Rambaut, A., Suchard, M.A., Xie, D., Drummond, A.J., 2014. Tracer 1.6. Available from <http://beast.bio.ed.ac.uk/Tracer>.

Refulio-Rodriguez, N.F., Olmstead, R.G., 2014. Phylogeny of Lamiidae. Am. J. Bot. 101, 287–299.

Rokas, A., Carroll, S.B., 2006. Bushes in the tree of life. PLoS Biol. 4, e352.

Ronquist, F., Huelsenbeck, J.P., 2003. MrBayes 3: Bayesian phylogenetic inference under mixed models. Bioinformatics 19, 1572–1574.

Shepherd, K.A., Wilson, P.G., 2007. Incorporation of the Australian genera *Halosarcia*, *Pachycornia*, *Sclerostegia* and *Tegicornia* into *Tecticornia* (Salicornioideae, Chenopodiaceae). Aust. Syst. Bot. 20, 319–331.

Shimodaira, H., 2002. An approximately unbiased test of phylogenetic tree selection. Syst. Biol. 51, 492–508.

Simmons, M.P., 2004. Independence of alignment and tree search. Mol. Phylogenet. Evol. 31, 874–879.

Soltis, D.E., Moore, M.J., Burleigh, J.G., Bell, C.D., Soltis, P.S., 2010. Assembling the angiosperm tree of life: progress and future prospects. Ann. Mo. Bot. Gard. 97, 514–526.

Stamatakis, A., 2014. RAxML version 8: A tool for phylogenetic analysis and post-analysis of large phylogenies. Bioinformatics, 1–2.

Steele, P.R., Hertweck, K.L., Mayfield, D., McKain, M.R., Leebens-Mack, J., Pires, J.C., 2012. Quality and quantity of data recovered from massively parallel sequencing: examples in Asparagales and Poaceae. Am. J. Bot. 99, 330–348.

Strand, A.E., Leebens-Mack, J.H., Milligan, B.G., 1997. Nuclear DNA-based markers for plant evolutionary biology. Mol. Ecol. 6, 113–118.

Straub, S.C.K., Parks, M., Weitemier, K., Fishbein, M., Cronn, R.C., Liston, A., 2012. Navigating the tip of the genomic iceberg: next-generation sequencing for plant systematics. Am. J. Bot. 99, 349–364.

Straub, S.C.K., Moore, M.J., Soltis, P.S., Soltis, D.E., Liston, A., Livshultz, T., 2014. Phylogenetic signal detection from an ancient rapid radiation: effects of noise reduction, long-branch attraction, and model selection in crown clade Apocynaceae. Mol. Phylogenet. Evol. 80, 169–185.

Sukumaran, J., Holder, M.T., 2010. DendroPy: a Python library for phylogenetic computing. Bioinformatics 26, 1569–1571.

Swofford, D.L. 2002. PAUP*. Phylogenetic Analysis Using Parsimony (* and Other Methods). Version 4. Sinauer Associates, Sunderland, Massachusetts.

Tank, D.C., Donoghue, M.J., 2010. Phylogeny and phylogenetic nomenclature of the Campanulidae based on an expanded sample of genes and taxa. Syst. Bot. 35, 425–441.

Timme, R.E., Kuehl, J.V., Boore, J.L., Jansen, R.K., 2007. A comparative analysis of the *Lactuca* and *Helianthus* (Asteraceae) plastid genomes: identification of divergent regions and categorization of shared repeats. Am. J. Bot. 94, 302–312.

Wang, H., Moore, M.J., Soltis, P.S., Bell, C.D., Brockington, S.F., Alexandre, R., Davis, C. C., et al., 2009. Rosid radiation and the rapid rise of angiosperm-dominated forests. Proc. Nation. Acad. Sci. USA 106, 3853–3858.

Weitemier, K., Straub, S.C., Cronn, R.C., Fishbein, M., Schmickl, R., McDonnell, A., Liston, A., 2014. Hyb-Seq: Combining target enrichment and genome skimming for plant phylogenomics. Applications in Plant Sciences 2. Published online 2014 August 29. doi: 10.3732/apps.1400042.

Western Australian Herbarium, 1998. FloraBase – the Western Australian Flora. Department of Parks and Wildlife. <http://florabase.dpaw.wa.gov.au/>.

Whitfield, J.B., Lockhart, P.J., 2007. Deciphering ancient rapid radiations. Trends Ecol. Evol. 22, 258–265.

Wiens, J.J., Fetzner, J.W., Parkinson, C.L., Reeder, T.W., 2005. Hylid frog phylogeny and sampling strategies for speciose clades. Syst. Biol. 54, 778–807.

Wolfe, K.H., Li, W.H., Sharp, P.M., 1987. Rates of nucleotide substitution vary greatly among plant mitochondrial, chloroplast, and nuclear DNAs. Proc. Nation. Acad. Sci. USA 84, 9054–9058.

Wurdack, K.J., Davis, C.C., 2009. Malpighiales phylogenetics: gaining ground on one of the most recalcitrant clades in the angiosperm tree of life. Am. J. Bot. 96, 1551–1570.

Xi, Z., Ruhfel, B.R., Schaefer, H., Amorim, A.M., Sugumaran, M., Wurdack, K.J., Endress, P.K., et al., 2012. Phylogenomics and a posteriori data partitioning resolve the Cretaceous angiosperm radiation Malpighiales. Proc. Nation. Acad. Sci. USA 109, 17519–17524.